Pergamon

Int. J. Mech. Sci. Vol. 36, No. 3, pp. 219–229, 1994

0020–7403/94 $6.00 + 0.00

UPPER-BOUND LIMIT ANALYSIS OF A RIGID–PLASTIC BODY WITH FRICTIONAL INTERFACES

H. S. Yu and S. W. Sloan
Department of Civil Engineering and Surveying, The University of Newcastle, NSW 2308, Australia

(*Received* 21 *December* 1992; *and in revised form* 24 *August* 1993)

Abstract—A finite element formulation of the upper-bound theorem for rigid–plastic solids, generalized to include interfaces with finite friction, is described. As proved by Collins [*J. Mech. Phys. Solids* **17**, 323 (1969)], the usual definition of a kinematically admissible velocity field is unnecessarily restrictive when the upper-bound theorem is applied to many practical problems. This paper shows that a relaxed inequality can be used successfully to derive upper bounds in the presence of Coulomb friction on interfaces, provided one considers a wide enough class of "admissible" velocity fields.

One of the major advantages of using a numerical formulation of the upper-bound theorem is that both complex loading geometry and inhomogeneous material behaviour can be easily dealt with. Using a suitable linear approximation of the yield surface, the application of the necessary boundary conditions, the plastic flow rule and the yield criterion lead to a large linear programming problem. The numerical procedure uses constant-strain triangular elements with the unknown velocities as the nodal variables. An additional set of unknowns, the plastic multiplier rates, is associated with each element. Kinematically admissible velocity discontinuities are permitted along specified planes within the finite element mesh. During the solution phase, an active set algorithm is used to solve the linear programming problem.

INTRODUCTION

Limit analysis is a powerful method for determining upper and lower bounds on the collapse loads of any structure. The upper-bound theorem is often used to assess the stability of engineering problems by modelling the material as rigid–plastic with an associated flow rule. It states that the loads, determined by equating the external rate of work to the internal rate of dissipation in an assumed deformation mode that satisfies (a) compatibility, (b) the flow rule, and (c) the velocity boundary conditions, are not less than the actual collapse load. A velocity field satisfying the above conditions is known as a kinematically admissible velocity field.

However, as noted by several writers, rigorous upper bounds cannot be generally obtained using the conventional upper-bound theorem when there is Coulomb friction on the interfaces (see, for example, the paper by Drucker [1]). Special conditions need to be satisfied in this case, and these are: (1) the coefficient of friction is zero; or (2) there is no relative motion or separation at the interface. According to the frictional theorem, the true limit load is bounded from below by the limit load which corresponds to zero friction on the interfaces. Conversely, it is bounded from above by the limit load for no relative motion at the interfaces. Physically, this means that the true limit load for problems with finite friction interfaces is bracketed by the limit loads which correspond to perfectly smooth and perfectly rough interfaces. For some stability problems in geotechnical engineering, the upper and lower bounds are not sensitive to the degree of roughness of the external loading boundary. This indicates that friction is of only secondary importance in the determination of the limit load. In some other cases, however, we find that there is a large difference between the bounds corresponding to rough and smooth interfaces and it is necessary to develop a method which can be used to assess the effect of any particular coefficient of friction.

In an attempt to develop a method to obtain an upper bound when the interface behaviour is governed by Coulomb's criterion, Collins [2] noted that the velocity boundary conditions do not need to be satisfied precisely for the upper bound inequality to be valid. In particular, he showed that if one chooses the "admissible" velocity field to be such that on

a planar interface the velocity component in the direction of the resultant surface traction is constant over the interface, then such a velocity field provides an upper bound to the total normal load in the presence of Coulomb friction.

The conventional way of determining upper bounds is to make use of a number of rigid block mechanisms. In these mechanisms, power is assumed to be dissipated only at the interfaces between adjacent blocks, and the geometry is optimized to yield the minimum dissipated power. A comprehensive discussion of the application of this type of approach for upper-bound limit analysis may be found in Ref. [3]. Although the rigid block method enjoys the advantage of being simple, it also has a number of drawbacks. Firstly, no volumetric plastic deformation is allowed to occur; secondly, problems with complex loading and complicated boundary conditions are difficult to deal with; and finally, it is not straightforward to model frictional materials because the dilation dictated by an associated flow rule often precludes the use of simple rigid block mechanisms.

In order to overcome these difficulties, finite element formulations of the upper-bound theorem have been used in recent years. These formulations permit rigorous upper bounds to be determined by using linear programming techniques and enjoy all of the advantages of the finite element method [4–6]. They permit plastic deformation to occur not only along velocity discontinuities, but also throughout the volume of the solid. In the formulation of Bottero *et al.* [5] and Sloan [6], a three-noded constant-strain triangular element is used to model the velocity field. Each node has two velocities and each element is associated with a set of nonnegative plastic multiplier rates. To ensure that the finite element formulation of the upper-bound theorem leads to a linear programming problem, it is necessary to express the yield criterion as a linear function of the stresses. For the Tresca or Mohr–Coulomb criterion, the yield surface is approximated by using an external linearization so that the solution obtained is a rigorous upper bound.

The main purpose of this paper is to present a finite element formulation of the upper-bound theorem which is generalized to include Coulomb friction. The generalized upper-bound theorem can be used to obtain overestimates of the total load in the presence of Coulomb friction provided one considers a wide enough class of "admissible" velocity fields. Numerical examples are given to illustrate the capability and effectiveness of the new procedure for computing rigorous upper bounds.

GENERALIZED UPPER-BOUND THEOREM

Collins [2] has proved that the velocity boundary conditions do not need to be satisfied precisely for the upper-bound inequality to be valid. Based on this important finding, he has also developed a generalized upper-bound theorem which can be used to solve many problems of practical interest. Although the main purpose of this paper is to present a numerical formulation of Collins' generalized upper-bound theorem, we also present a summary of this theorem for the sake of completeness.

Consider a volume V of rigid–plastic solid and assume its surface is divided into two parts. On one part S_f, some or all of the traction components are prescribed. The rest of the surface S_u corresponds to the frictional interface which may be subject to certain types of velocity conditions.

Let u^* be any piecewise-continuous velocity field defined over V which gives rise to a strain-rate field e_{ij}^*. The corresponding plastic stress field σ_{ij}^*, related to e_{ij}^* through the flow rule, will not in general be self-equilibrated. If σ_{ij} is the actual failure stress field which is self-equilibrated, then from the maximum work inequality we have:

$$(\sigma_{ij} - \sigma_{ij}^*)e_{ij}^* \leqslant 0 \tag{1}$$

throughout V, so that:

$$\int_V \sigma_{ij} e_{ij}^* \, \mathrm{d}V \leqslant \int_V \sigma_{ij}^* e_{ij}^* \, \mathrm{d}V. \tag{2}$$

This inequality holds if the yield function is convex and identical to the plastic potential [7]. Using the principle of virtual work and Eqn (2) leads to the following well-known

upper-bound inequality:

$$\int_{S_u} T_i u_i^* \, dS_u \leqslant \int_V \sigma_{ij}^* e_{ij}^* \, dV - \int_{S_f} T_i u_i^* \, dS_f . \tag{3}$$

Note that the volume integral is assumed to include contributions to the energy dissipation rate from any internal velocity discontinuities. This is the standard proof of the upper-bound theorem. Since the inequality (3) holds irrespective of whether u^* is compatible with the actual velocity conditions on the frictional interface S_u, u^* does not have to be a kinematically admissible velocity field.

Let us assume u_n^* and u_t^* are the normal and tangential components of u^* on S_u, which is assumed to be planar for the present. In addition, let T_n and T_t represent the corresponding traction components. The general Coulomb's law for the frictional interface may be expressed as:

$$| T_t | = c_w - s_n T_n \tan \phi_w, \tag{4}$$

where $s_n = 1$ if T_n points out of the body and $s_n = -1$ if T_n points into the body. The quantities c_w and ϕ_w denote the cohesion and friction angle on the interface, and tensile stresses are assumed to be positive. Using the above equation, we can write the upper-bound inequality (3) as:

$$\int_{S_u} (s_n u_n^* - s_t s_n u_t^* \tan \phi_w) T_n \, dS_u \leqslant \int_V \sigma_{ij}^* e_{ij}^* \, dV - \int_{S_f} T_i u_i^* \, dS_f - s_t \int_{S_u} c_w u_t^* \, dS_u, \tag{5}$$

where the sign s_t is defined so that $| T_t | = s_t T_t$ and $s_t = \pm 1$. In other words, $s_t = 1$ if T_t has a clockwise direction around the boundary of the body and $s_t = -1$ otherwise. The right-hand side of this inequality can be evaluated for any trial velocity field u^* since c_w is given.

Suppose now we are interested in obtaining an overestimate of the total normal load on S_u, i.e. $\int_{S_u} T_n \, dS_u$, which could be tensile (if $s_n = 1$) or compressive (if $s_n = -1$). Inequality (5) will provide such an overestimate for any trial velocity field u^* which has the property that:

$$s_n u_n^* - s_t s_n u_t^* \tan \phi_w = C \tag{6}$$

on S_u, where C is a positive constant. In general this will not be a kinematically admissible velocity field since the actual boundary condition may be different (e.g. for a rigid footing problem, the normal component of velocity should be constant).

Thus it would appear that our criterion in choosing the trial velocity field should not be that it satisfies the actual boundary conditions, but rather that it should satisfy Eqn (6) to give an upper bound on the "quantity of interest". The procedure differs from the usual one only in the velocity condition imposed on S_u. We now show how the generalized upper-bound theorem may be incorporated in a finite element formulation.

FINITE ELEMENT FORMULATION

Figure 1 shows the three-noded triangle element used in the finite element formulation of the upper-bound theorem. Each element has six nodal velocities and p plastic multiplier rates (where p is the number of sides in the linearized yield polygon). The former quantities vary linearly over each triangle according to:

$$u = \sum_{i=1}^{3} N_i u_i; \quad v = \sum_{i=1}^{3} N_i v_i, \tag{7}$$

where (u_i, v_i) are the nodal velocities in the x- and y-directions, respectively, and N_i are linear shape functions. To obtain a linear programming problem, it is necessary to approximate the Mohr–Coulomb criterion by a yield criterion which is linear in the stresses. For the upper-bound analysis, the linearized yield function must contain the Mohr–Coulomb function so that the important bounding property of the calculation is retained. As shown in Fig. 2, a polygonal approximation is used which has p sides of equal length and

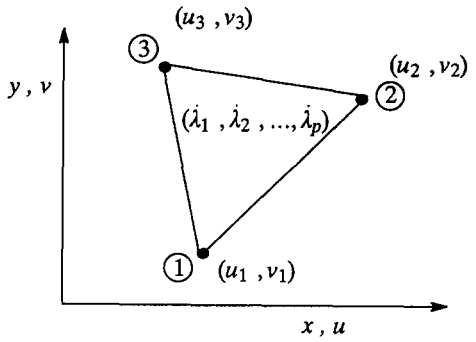

FIG. 1. A three-noded triangle element.

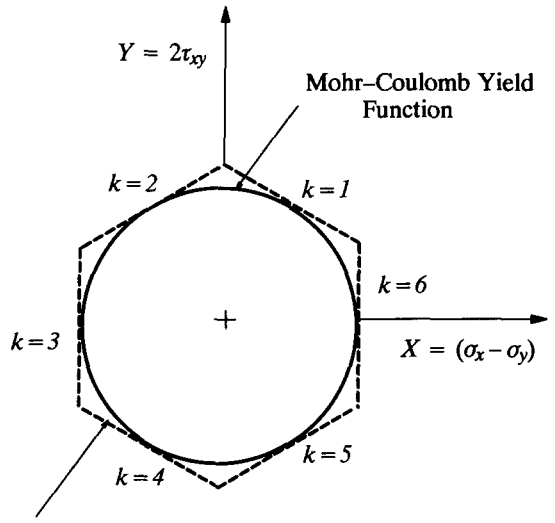

FIG. 2. External linear approximation to Mohr–Coulomb yield function ($p = 6$).

is defined by:

$$F_k = A_k\sigma_x + B_k\sigma_y + C_k\tau_{xy} - 2c\cos\phi = 0, \tag{8}$$

where:

$$A_k = \cos\frac{2k\pi}{p} + \sin\phi; \quad B_k = \sin\phi - \cos\frac{2k\pi}{p}; \quad C_k = 2\sin\frac{2k\pi}{p}, \tag{9}$$

and $k = 1, 2, 3 \ldots, p$. The quantities ϕ and c denote the friction angle and cohesion respectively.

For this linearized yield function, an associated flow rule gives the plastic strain rates throughout each triangle as:

$$\dot{\varepsilon}_x = \frac{\partial u}{\partial x} = \sum_{k=1}^{p} \dot{\lambda}_k \frac{\partial F_k}{\partial \sigma_x} = \sum_{k=1}^{p} \dot{\lambda}_k A_k, \tag{10}$$

$$\dot{\varepsilon}_y = \frac{\partial v}{\partial y} = \sum_{k=1}^{p} \dot{\lambda}_k \frac{\partial F_k}{\partial \sigma_y} = \sum_{k=1}^{p} \dot{\lambda}_k B_k, \tag{11}$$

$$\dot{\gamma}_{xy} = \left(\frac{\partial v}{\partial x} + \frac{\partial u}{\partial y}\right) = \sum_{k=1}^{p} \dot{\lambda}_k \frac{\partial F_k}{\partial \tau_{xy}} = \sum_{k=1}^{p} \dot{\lambda}_k C_k, \tag{12}$$

where $\dot{\lambda}_k$ is the positive plastic multiplier rate associated with the kth side of the yield polygon. Differentiating the linear expressions for velocities and substituting in the above equations, the flow rule equality constraints are obtained as:

$$\mathbf{A}_{11}\mathbf{u} + \mathbf{A}_{12}\dot{\boldsymbol{\lambda}} = \mathbf{b}_1, \tag{13}$$

with $\mathbf{u}^T = \{u_1, v_1, u_2, v_2, u_3, v_3\}$, $\mathbf{b}_1^T = \{0, 0, 0\}$, $\dot{\boldsymbol{\lambda}}^T = \{\dot{\lambda}_1, \ldots, \dot{\lambda}_p\}$. The matrix $\mathbf{A}_{11}$ is a function of the nodal coordinates which can be expressed by:

$$\mathbf{A}_{11} = \frac{1}{2A}\begin{bmatrix} b_1 & 0 & b_2 & 0 & b_3 & 0 \\ 0 & c_1 & 0 & c_2 & 0 & c_3 \\ c_1 & b_1 & c_2 & b_2 & c_3 & b_3 \end{bmatrix},$$

where:

$$b_1 = y_2 - y_3; \quad c_1 = x_3 - x_2,$$

$$b_2 = y_3 - y_1; \quad c_2 = x_1 - x_3,$$

$$b_3 = y_1 - y_2; \quad c_3 = x_2 - x_1,$$

$$A = \tfrac{1}{2}\,|(x_1 - x_3)(y_2 - y_3) - (x_3 - x_2)(y_3 - y_1)|,$$

in which (x_i, y_i) denote the coordinates for node i in an element. The matrix $\mathbf{A}_{12}$ is a function of the coefficients A_k, B_k and C_k. The explicit expression for $\mathbf{A}_{12}$ is:

$$\mathbf{A}_{12} = \begin{bmatrix} -A_1 & -A_2 & \cdots & -A_p \\ -B_1 & -B_2 & \cdots & -B_p \\ -C_1 & -C_2 & \cdots & -C_p \end{bmatrix}.$$

In addition to general plastic deformation throughout the volume of the solid, the upper-bound formulation permits localized plastic deformation along velocity discontinuities. A typical segment of a velocity discontinuity, defined by the nodal pairs (1, 2) and (3, 4), is shown in Fig. 3. For an arbitrary pair of nodes which have identical coordinates but which lie on opposite sides of a discontinuity, the jumps in tangential and normal velocity are given by:

$$u_t = \cos\theta(u_2 - u_1) + \sin\theta(v_2 - v_1), \tag{14}$$

$$u_n = \sin\theta(u_1 - u_2) + \cos\theta(v_2 - v_1), \tag{15}$$

where (u_1, v_1) and (u_2, v_2) are nodal velocities and θ is the inclination of the discontinuity to the x-axis. In order to preserve a linear constraint matrix in the formulation, it is necessary to specify the sign s of the tangential velocity such that $|u_t| = su_t$ and $s = \pm 1$. Applying the sign condition $su_t \geqslant 0$ and substituting Eqn (14) gives rise to an inequality constraint of the form:

$$\mathbf{a}_2\mathbf{u} \leqslant \mathbf{b}_2, \tag{16}$$

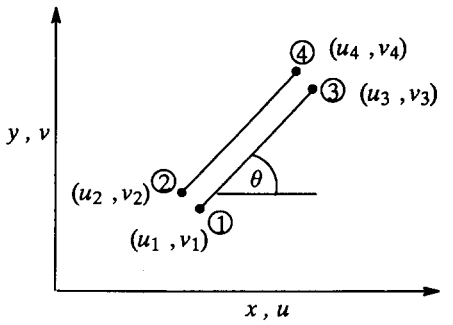

FIG. 3. Velocity discontinuity.

where $\mathbf{u}^T = \{u_1, v_1, u_2, v_2\}$, $\mathbf{b}_2 = 0$, and $\mathbf{a}_2$ is a function of s and θ which can be expressed as follows:

$$\mathbf{a}_2 = [s\cos\theta, s\sin\theta, -s\cos\theta, -s\sin\theta].$$

This type of constraint must be enforced at each nodal pair on a discontinuity so that the sign condition is satisfied everywhere along its length. As well as satisfying a sign condition, the discontinuity velocities must also obey the flow rule. The associated form of Mohr–Coulomb plasticity stipulates that $u_n = |u_t| \tan\phi$, which can be expressed as:

$$\mathbf{a}_3\mathbf{u} = \mathbf{b}_3, \tag{17}$$

where $\mathbf{u}^T = \{u_1, v_1, u_2, v_2\}$, $\mathbf{b}_3 = 0$, and the matrix $\mathbf{a}_3$ contains terms which are functions of θ according to:

$$\mathbf{a}_3 = [-m_1, -m_2, m_1, m_2],$$

with:

$$m_1 = s\tan\phi\cos\theta + \sin\theta,$$

$$m_2 = s\tan\phi\sin\theta - \cos\theta.$$

These conditions are again enforced at each pair of nodes on the discontinuity.

The last set of constraints to be imposed on the unknowns arises from the velocity boundary conditions on S_f and S_u. For a specified node i, the boundary conditions on S_f may be written as:

$$\mathbf{a}_4\mathbf{u} = \mathbf{b}_4, \tag{18}$$

where $\mathbf{a}_4$ is the identity matrix, $\mathbf{u}^T = \{u_i, v_i\}$ and $\mathbf{b}_4^T = \{\delta_1, \delta_2\}$.

To incorporate the generalized upper-bound theorem, an additional set of constraints on the unknown velocity field along the frictional interface S_u needs to be imposed. In order to obtain an upper-bound to the total normal load along the interface, the constraint defined by Eqn (6) must be satisfied. This constraint needs to be imposed at all nodes along the interface so that it is satisfied along the entire boundary. Thus for each node i, we have:

$$\mathbf{a}_5\mathbf{u} = \mathbf{b}_5, \tag{19}$$

where $\mathbf{a}_5 = \{(-s_n\sin\theta_w - s_t s_n\tan\phi_w\cos\theta_w), (s_n\cos\theta_w - s_t s_n\tan\phi_w\sin\theta_w)\}$, θ_w is the inclination of the interface to the x-axis, $\mathbf{u}^T = \{u_i, v_i\}$ and $\mathbf{b}_5 = C$.

The constraints that need to be imposed on the velocity field to ensure that it is kinematically admissible (in the modified sense) have now been covered. To complete the description of the upper-bound technique, we now need to express the objective function, which corresponds to the internal dissipated power, in terms of the unknowns.

The power dissipated along a velocity discontinuity of length L may be shown to be

$$P_d = \int_L c|u_t|\,dL = sc\int_L u_t\,dL = \tfrac{1}{2}scL[\cos\theta(u_2 + u_4 - u_1 - u_3) + \sin\theta(v_2 + v_4 - v_1 - v_3)], \tag{20}$$

where it is assumed that the segment is defined by the nodal pairs (1, 2) and (3, 4). This may be written as:

$$P_d = \mathbf{c}_1^T\mathbf{u}, \tag{21}$$

in which $\mathbf{u}^T = \{u_1, v_1, \ldots, u_4, v_4\}$ and the objective function coefficients $\mathbf{c}_1$ can be expressed in terms of s, c, L and θ as follows:

$$\mathbf{c}_1^T = \tfrac{1}{2}scL[-\cos\theta, -\sin\theta, \cos\theta, \sin\theta, -\cos\theta, -\sin\theta, \cos\theta, \sin\theta].$$

In the numerical implementation of the upper-bound theorem, we also permit power to be dissipated by plastic deformation throughout each triangle. By substituting the equations for the plastic strain rates and linearized yield criterion into the fundamental definition

of plastic power, the power dissipated internally may be expressed as:

$$P_t = 2c \cos \phi A \sum_{k=1}^{p} \dot{\lambda}_k, \tag{22}$$

where it is assumed that the properties c and ϕ are uniform over the triangle of area A. Alternatively, we may write:

$$P_t = \mathbf{c}_2^T \dot{\boldsymbol{\lambda}}, \tag{23}$$

in which the objective function coefficients $\mathbf{c}_2$ are given by:

$$\mathbf{c}_2^T = [2cA \cos \phi, 2cA \cos \phi, \ldots, 2cA \cos \phi].$$

The contribution to the dissipated power from the cohesion of the interface S_u can be expressed as:

$$P_w = -s_t c_w \int_{S_u} u_t^* \, dS_u = -\tfrac{1}{2} s_t c_w L_w \cos \theta_w (u_1 + u_2) - \tfrac{1}{2} s_t c_w L_w \sin \theta_w (v_1 + v_2), \tag{24}$$

where it is assumed that the interface is of length L_w and defined by nodes 1 and 2 and θ_w denotes the angle between the interface and the x-axis. This equation can be written in the following form:

$$P_w = \mathbf{c}_3^T \mathbf{u}, \tag{25}$$

where $\mathbf{c}_3^T$ is a function of s_t, c_w, L_w and θ_w while $\mathbf{u}^T = \{u_1, v_1, u_2, v_2\}$.

The various constraint matrices and objective function coefficients, defined by Eqns (13), (16)–(19), (21), (23) and (25), may be assembled by the usual rules to yield the following upper-bound linear programming problem:

$$\text{Minimize} \quad (\mathbf{C}_1^T + \mathbf{C}_3^T)\mathbf{X}_1 + \mathbf{C}_2^T \mathbf{X}_2 \tag{26}$$

$$\text{Subject to} \quad \mathbf{A}_{11}\mathbf{X}_1 + \mathbf{A}_{12}\mathbf{X}_2 = \mathbf{B}_1, \tag{27}$$

$$\mathbf{A}_2 \mathbf{X}_1 \leqslant \mathbf{B}_2, \tag{28}$$

$$\mathbf{A}_3 \mathbf{X}_1 = \mathbf{B}_3, \tag{29}$$

$$\mathbf{A}_4 \mathbf{X}_1 = \mathbf{B}_4, \tag{30}$$

$$\mathbf{A}_5 \mathbf{X}_1 = \mathbf{B}_5, \tag{31}$$

$$\mathbf{X}_2 \geqslant \mathbf{0}, \tag{32}$$

where, for a mesh of N nodes and E triangles with $M = pE$, $\mathbf{X}_1^T = \{u_1, v_1, \ldots, u_N, v_N\}$ is the global vector of unknown velocities and $\mathbf{X}_2^T = \{\dot{\lambda}_1, \ldots, \dot{\lambda}_M\}$ is the global vector of unknown plastic multiplier rates. A detailed discussion of efficient strategies for solving this type of optimization problem can be found in Ref. [6] and will not be repeated here. It is merely noted that the steepest edge active set algorithm, as developed by Sloan [8], has proved to be very effective when it is applied to the dual of the above linear programming problem.

APPLICATIONS

The numerical upper-bound procedure outlined in the previous sections will now be used to investigate the effect of base roughness on the bearing capacity of a footing resting on a cohesive–frictional soil with weight. As noted by Chen [3], the base roughness has a significant effect on the bearing capacity of a footing when the self-weight of the soil is taken into account. The inclusion of self-weight and base friction is difficult in a traditional upper-bound calculation and this question still remains unsolved.

In the experiments reported by Ko and Davidson [9], it is observed that smooth glass footings in sand fail according to the Hill type of mechanism since two symmetrical wedges beneath the footing are developed. Footings with rough sandpaper interfaces, on the other hand, seem to fail according to the Prandtl type of mechanism as only a central wedge

beneath the footing is developed. Thus, two contrasting failure mechanisms are observed in their experiments, depending on whether the footing is almost perfectly smooth or almost perfectly rough. This observation leads us to believe that neither the Hill mechanism nor the Prandtl mechanism can be expected to give an accurate estimate of the bearing capacity for a footing with base friction. To quantify the effect of the footing roughness on the ultimate bearing capacity, the experimental work of Meyerhof [10] suggests that the bearing capacity of a smooth footing on the surface of a cohesionless soil should be about one-half of that for a rough footing.

To quantify the effect of the footing roughness, the finite element formulation of the upper-bound theorem is used with the mesh shown in Fig. 4a and b. This mesh comprises 290 nodes and 512 triangular elements. It is well-known that the bearing capacity of a footing depends not only on the mechanical properties of the soil (friction angle and cohesion), but also on the physical characteristics of the footing (footing geometry and roughness). Indeed, Cox [11] has shown that for a smooth surface footing resting on a Mohr–Coulomb soil with no surcharge, the fundamental parameters associated with the stress characteristic equations are the friction angle ϕ and $G = \gamma B/2c$, where c is the cohesion, γ is the unit weight of soil and B is the width of the footing. If G is small, then the soil behaves essentially as a cohesive weightless medium. If G is large, the soil's weight rather than its cohesion is the principal source of bearing strength. For a surface footing with no surcharge, the dimensionless bearing capacity q_0/c depends only on the angle of internal friction of the soil ϕ, the dimensionless soil weight parameter G and the footing base friction angle ϕ_w. In our study, a value of 30° is used to represent the soil friction angle in the analysis and the effect of self-weight is investigated by using different values of G. A perfectly rough footing can be modelled by setting $\phi_w = \phi$ and $c_w = c$, while the case $\phi_w = 0$ and $c_w = 0$ represents a perfectly smooth footing. In practice, a footing with base friction typically has $0 < \phi_w < \phi$ and $0 < c_w < c$.

The effect of the base friction on the bearing capacity of a footing is shown in Fig. 5. For the case when G is very small, such as $G = 0.1$, the curves are characterized by a rising portion followed by a relatively flat section. At the intersection of the rising portion and the

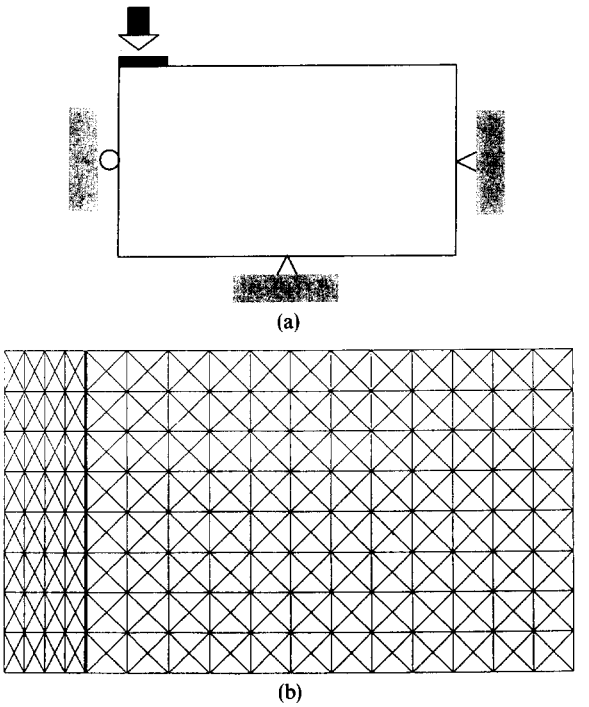

FIG. 4. (a) Boundary conditions and (b) finite element mesh used for modelling a rigid strip footing on a cohesive–frictional soil.

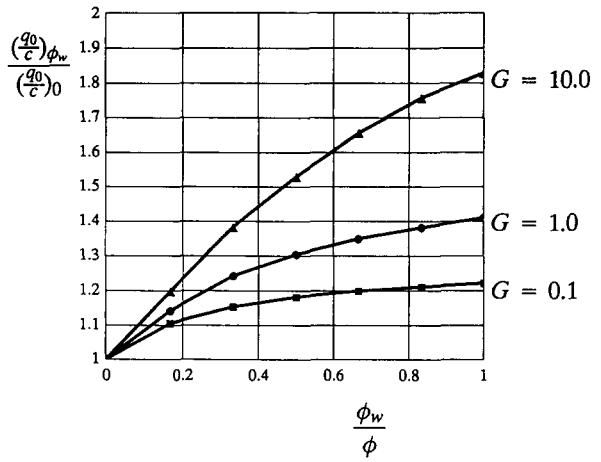

FIG. 5. The effect of footing roughness on the bearing capacity.

flat section, the base friction is just sufficient to restrain any sliding motion between the base and the adjacent soil. Any increase in the base friction angle beyond this point will not yield a significant increase in the bearing capacity. The results presented here indicate that a rather modest value of base friction is sufficient to create an essentially perfectly rough condition. For relatively large values of G, base friction seems to have a significant effect on the bearing capacity. This effect is less pronounced when $G = 0.1$ or $G = 1.0$. This is to be expected, since Prandtl's solution for a weightless soil ($G = 0.0$) has been shown to be independent of base friction. For the case when $G = 10.0$, the bearing capacity is found to increase continuously with the base friction angle. Indeed, the bearing capacity of a rough footing is nearly twice that of a smooth footing when the friction angle is equal to 30° and $G = 10.0$. For most practical problems, values of G can normally be expected to range from 0.1 to 1.0, and within this range the effect of the footing roughness may increase the bearing capacity by up to 50%.

The numerical velocity field and deformed mesh for a realistic case when the footing is neither perfectly smooth nor perfectly rough, with $\phi = 30°$ and $\phi_w = 15°$, are plotted in Figs 6 and 7 for $G = 1.0$. It is evident from Fig. 6 that the numerical velocity field appears to be a combination of the Hill and the Prandtl fields. Generally speaking, the size of the plastically deforming zone, and therefore the bearing capacity, increases with the angle of base friction. In particular, it is found that the numerically determined velocity field for a perfectly smooth footing closely agrees with that predicted by the Hill mechanism. The numerical velocity field for a perfectly rough footing, on the other hand, is very similar to the Prandtl field. In conclusion, the experimental observations made by Ko and Davidson [9], regarding the failure mechanism, and Meyerhof [10], regarding the effect of footing roughness on the bearing capacity, are strongly substantiated by the numerical upper-bound results presented in this paper.

The perfectly rough case

There are two ways to calculate an upper bound on the collapse load for a perfectly rough footing. In the first approach, we can use the numerical method proposed in this paper and assume $\phi_w = \phi$ and $c_w = c$. On physical grounds, it is obvious that the maximum shear strength at the soil–footing interface cannot exceed the maximum shear strength of the soil itself. Since the flow rule is not violated, the generalized upper-bound theorem remains valid and the solution obtained is a rigorous upper bound on the true collapse load. Alternatively the collapse load for a perfectly rough footing is calculated by using the conventional upper-bound theorem and prescribing a zero horizontal displacement for all nodes on the soil–footing interface. To compare the results obtained from these two different approaches, both of these methods have been used to analyse a rough footing problem.

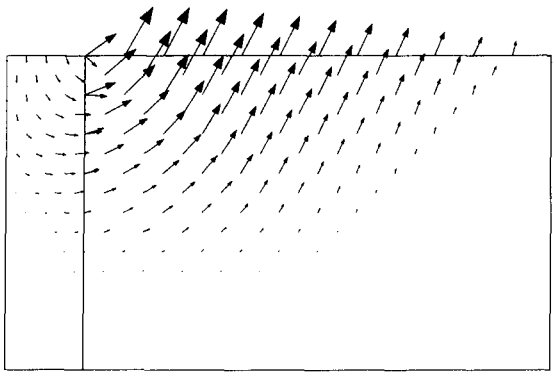

FIG. 6. Numerical velocity field for rigid strip footing on cohesive–frictional soil ($\phi = 30$, $\phi_w = 15$).

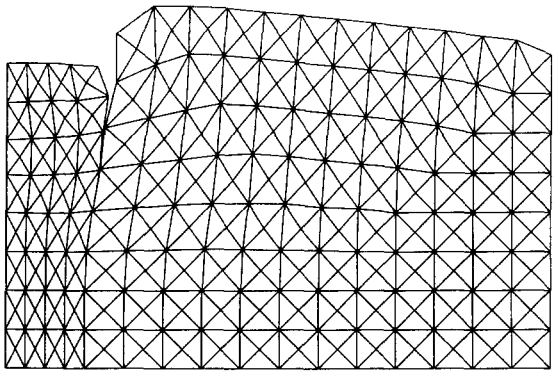

FIG. 7. Deformed mesh for rigid strip footing on cohesive–frictional soil ($\phi = 30$, $\phi_w = 15$).

TABLE 1. THE CALCULATED BEARING CAPACITIES FOR A PERFECTLY ROUGH STRIP FOOTING IN A COHESIVE-FRICTIONAL SOIL

Mesh	Methods	$G = 10$	$G = 1.0$	$G = 0.1$
Coarse	Conventional	350.5	75.5	45.0
	Generalized	311.4	71.9	43.9
Fine	Conventional	282.9	65.5	39.7
	Generalized	262.3	63.6	39.2

In addition to the mesh shown in Fig. 4, a finer mesh with 958 nodes and 1792 elements is also used in the calculation so that the sensitivity of the results to the level of discretization can be investigated. The friction angle of the soil is assumed to be 30° and values of 10.0, 1.0, 0.1 have been used to represent the self-weight parameter G. The results are summarized in Table 1. In general, it is found that the numerical solutions compare favourably with the approximate upper-bound solutions obtained from the Prandtl type of mechanisms of Chen [3]. It can be seen from this table that the results obtained using the generalized upper-bound method are less than those obtained by the conventional upper-bound theorem. This suggests that the generalized upper-bound theorem can be used to give better upper bounds when a perfectly rough interface needs to be modelled. The improvement is most pronounced when a coarse mesh is used in the calculation. When a sufficiently fine mesh is employed, the difference between the generalized upper-bound theorem and the conventional upper-bound theorem becomes smaller. As expected, the results between these two approaches are very similar when G is small, since the effect of the roughness of the soil–footing interface is less significant for these cases.

CONCLUSION

A finite element formulation of the generalized upper-bound theorem, which can be used to obtain upper bounds in the presence of frictional interfaces, has been developed. The generalized upper-bound theorem is based on the fact that the velocity boundary condition does not need to be satisfied precisely for the upper-bound inequality to be valid. Consequently, this inequality can be applied to a wide class of problems. The relaxed inequality method is simple to use and differs little from the conventional upper-bound theorem. The new procedure has been used to quantify the effect of base friction on the bearing capacity of a rigid footing to highlight its potential for solving many practical problems of interest.

Acknowledgement—The work reported in this paper forms part of a general research programme on geotechnical stability analysis in the Department of Civil Engineering at the University of Newcastle. This research is supported by the Australian Research Council (ARC) and the authors are thankful for this support.

REFERENCES

1. D. C. DRUCKER, Coulomb friction, plasticity and limit loads. *J. Appl. Mech. ASME* **21**, 71 (1954).
2. I. F. COLLINS, The upper bound theorem for rigid/plastic solids generalized to include Coulomb friction. *J. Mech. Phys. Solids* **17**, 323 (1969).
3. W. F. CHEN, *Limit Analysis and Soil Plasticity*. Elsevier, Amsterdam (1975).
4. E. ANDERHEGGEN and H. KNOPFEL, Finite element limit analysis using linear programming. *Int. J. Solids Struct.* **8**, 1413 (1972).
5. A. BOTTERO, R. NEGRE, J. PASTOR and S. TURGEMAN, Finite element method and limit analysis theory for soil mechanics problems. *Comp. Meth. Appl. Mech. Engng* **22**, 131 (1980).
6. S. W. SLOAN, Upper bound limit analysis using finite elements and linear programming. *Int. J. Numer. Analysis Meth. Geomech.* **13**, 263 (1989).
7. R. HILL, *The Mathematical Theory of Plasticity*. Oxford University Press, Oxford (1951).
8. S. W. SLOAN, A steepest edge active set algorithm for solving sparse linear programming problems. *Int. J. Numer. Meth. Engng* **26**, 2671 (1988).
9. H. Y. KO and L. W. DAVIDSON, Bearing capacity of footings in plane strain. *J. Soil Mech. Found. Div. ASCE* **99**, 1 (1973).
10. G. G. MEYERHOF, Influence of roughness of base and ground-water conditions on the ultimate bearing capacity of foundations. *Geotechnique* **5**, 227 (1955).
11. A. D. COX, Axially symmetric plastic deformation in soils—II. Indentation of ponderable soils. *Int. J. Mech. Sci.* **4**, 371 (1963).